

**UCLA**

**UCLA Previously Published Works**

**Title**

Electrophysiological Approaches to Studying the Suprachiasmatic Nucleus

**Permalink**

<https://escholarship.org/uc/item/2j7384r8>

**Authors**

Michel, Stephan  
Nakamura, Takahiro J  
Meijer, Johanna H  
[et al.](#)

**Publication Date**

2021

**DOI**

10.1007/978-1-0716-0381-9\_23

**Copyright Information**

This work is made available under the terms of a Creative Commons Attribution License, available at <https://creativecommons.org/licenses/by/4.0/>

Peer reviewed



## Electrophysiological Approaches to Studying the Suprachiasmatic Nucleus

Stephan Michel, Takahiro J. Nakamura, Johanna H. Meijer, and Christopher S. Colwell

### Abstract

In mammals, the part of the nervous system responsible for most circadian behavior can be localized to a bilaterally paired structure in the hypothalamus known as the suprachiasmatic nucleus (SCN). Understanding the mammalian circadian system will require a detailed multilevel analysis of neural SCN circuits *ex vivo* and *in vivo*. Many of the techniques and approaches that are used for the analysis of the circuitry driving circadian oscillations in the SCN are similar to those employed in other brain regions. There is, however, one fundamental difference that needs to be taken into consideration, that is, the physiological, cell, and molecular properties of SCN neurons vary with the time of day. In this chapter, we will consider the preparations and electrophysiological techniques that we have used to analyze the SCN circuit focusing on the acute brain slice and intact, freely moving animal.

**Key words** Biological clock, Brain slice, Circadian, *In vivo* electrophysiology, Neural activity rhythms, Suprachiasmatic nucleus

---

### 1 Introduction

The ability of the SCN neural population to generate neural activity rhythms in isolation from the rest of the organism has been documented in numerous studies using an acute brain slice preparation [1, 2]. Data obtained from the brain slice provided critical evidence in support of the view that the generation of circadian electrical activity rhythms is not a neural network property in which synaptic feedback information from one neuron to the other is required for the presence of circadian rhythmicity. Instead, these studies are all consistent with the idea that many SCN neurons are stable, self-sustained oscillators that have the intrinsic capacity to generate circadian rhythms. That said, there is evidence that circuit properties contribute to the robustness and precision of SCN circadian oscillations [3, 4]. *In vivo* recording of SCN neural activity has been critical to determine how these neural rhythms are influenced by

the intact input [5–7] and, for example, has established how the behavioral state of the organism can feedback to regulate SCN activity [8]. One of the critical challenges of ongoing work is the development of an understanding of how a molecular feedback loop occurring at the level of transcription and translation interacts with the neuronal plasmalemmal membrane to produce physiological rhythms. It is not known how the molecular feedback loop drives the electrical rhythm in membrane processes, and this is a critical question for the field [2, 9]. In addition, there is a growing body of evidence that disruptions in the SCN neural activity rhythms are common in aging and diseases of the nervous system [10, 11]. Understanding the underlying mechanisms could explain how pathological processes alter the electrical output as well as lead to the development of possible treatment strategies.

The techniques and approaches that are used for the analysis of the circuit driving circadian oscillations in the SCN are similar to those used in other brain regions. There is one fundamental difference that needs to be taken into consideration, that is, the physiological, cell, and molecular properties of SCN neurons vary with time of day. These cells continue to oscillate in the dish so the daily cycle needs to be a consideration independent on whether the experiments are conducted in vivo, using ex vivo brain slices or in cultured explants or neurons. For example, circadian oscillations in  $\gamma$ -aminobutyric acid (GABA)-mediated synaptic transmission in both presynaptic release and postsynaptic responses have been described [12, 13]. Moreover, the neurons show spontaneous circadian oscillations in electrical activity driven, at least in part, by daily rhythms in intrinsic membrane properties in these cells [2, 14]. Signaling pathways within these cells oscillate, including dynamic changes of cytosolic  $\text{Ca}^{2+}$  and cyclic adenosine monophosphate/protein kinase-A (cAMP/PKA) activity [15–18]. Since circadian oscillations are generated by transcriptional–translational feedback loops, a wide range of genes are rhythmically regulated including those involved in secretion and synaptic transmission critical for circuits. So for the circadian system, time of day is a critical variable that always has to be considered. The extent to which these circadian variations influence other brain circuits is not yet known, although it is well established that molecular oscillations in clock gene expression are widespread within the nervous system [19–22].

Given that the SCN system comprises a circuit of endogenous oscillators that is synchronized to light, the external lighting conditions for all of these experiments need to be carefully considered. When animals are in a light–dark (LD) cycle, they may exhibit day–night variation in a number of parameters. These rhythms are influenced by the internal circadian system and by the direct effects of light and dark. Consequently, a rhythm recorded under these conditions can be considered a diurnal but not necessarily a

circadian rhythm, that is, an internally generated rhythm. An important—though little employed—experiment is to reverse the timing of the LD cycle and show that the resulting rhythm follows the change in the light schedule. This confirms that the diurnal rhythm is at least driven by the environmental conditions but does not necessarily address whether the rhythm has an endogenous origin. In order to isolate the endogenous circadian component driving these differences, it is necessary to hold the organism in constant conditions, that is, constant dark (DD) and constant temperature. In the intact system, the animal's behavior and locomotor activity can be followed with the convention that the onset of activity for a nocturnal organism is defined as circadian time (CT) 12. While activity onset is a convenient and reliable way to follow the endogenous rhythm, other robust circadian outputs could be used including body temperature or heart rate. For generation of brain slices, the LD cycle in which the animal was held prior to being sacrificed is an excellent predictor of the activity phase of the SCN population.

For the rest of this chapter, we will consider the techniques used to analyze the SCN circuit focusing on acute brain slice and *in vivo* recordings. The materials, methods, and approaches in employing each of these techniques including a short description of the advantages and disadvantages will be described. Certainly, other techniques can be usefully applied, but we will focus on the preparations and techniques with which we have working experience.

---

## 2 Materials

### 2.1 *Materials for Brain Slice*

1. Solutions (concentration in mM): Artificial cerebrospinal fluid (ACSF): NaCl 130, NaHCO<sub>3</sub> 26, KCl 3, MgCl<sub>2</sub> 2, NaH<sub>2</sub>PO<sub>4</sub> 1.25, CaCl<sub>2</sub> 2, glucose 10. Modified ACSF (for vibratome slicing): same as ACSF except MgCl<sub>2</sub> 5, CaCl<sub>2</sub> 1. The solutions are prepared the day before the experiment, gassed with 95% O<sub>2</sub> 5% CO<sub>2</sub> (pH adjusted to 7.2–7.4, osmolality 290–300 mOsm) and kept at 4 °C. For long-term recording of slices (>24 h), gentamycin (5 µg/ml) is added to the ACSF.
2. Anesthetic agents (4% isoflurane) and anesthetic chamber.
3. Sterilized dissection tools, guillotine for decapitation, dissecting scissors, forceps, spatulas, and razor blade for trimming.
4. Slice cutting: vibratome (e.g., Microslicer, DSK Model 1500E, Ted Pella, Redding, CA, USA or Leica VT 1200S, Wetzlar, Germany) or tissue chopper (e.g., McIlwain Tissue Chopper, The Mickle Laboratory Engineering, Guildford, UK).

5. Electrophysiological recording equipment (patch clamp): vibration isolated table (e.g., TMC, Peabody, MA, USA), Faraday cage, manipulator (e.g., Sutter, Novato, CA, USA or Luig&Neumann, Ratingen, Germany), slice recording chamber (e.g., Warner Series 20, Hamden, CT, USA), gravity fed perfusion control (e.g., ALA perfusion systems, Farmingdale, NY, USA), gas (5 % CO<sub>2</sub>/95% O<sub>2</sub>) control and distribution, vacuum control, patch amplifier (e.g., Axon Axopatch 200B or HEKA EPC10, Lambrecht, Germany), control software (e.g., Axon pClamp or HEKA Patchmaster).
6. Electrophysiological recording equipment (long-term multi-unit recording): vibration damped table, Faraday cage, temperature-controlled perfusion chamber, water bath, perfusion pump, vacuum control, extracellular amplifier (e.g., 5113 Low Noise Voltage Preamplifier, Signal Recovery, Oak Ridge, TN, USA), digitizer (e.g., CED 1401 with Spike2 software, CED, Cambridge, England).
7. Infrared (IR)-patch: Upright water immersion microscope equipped with IR-DIC (e.g., Zeiss Axioskop FS2plus, Carl Zeiss, Göttingen, Germany) or Olympus BX51W, Olympus, Center Valley, PA, USA), IR-camera (e.g., Hamamatsu C2400 or Watec, 902H, Newburgh NY, USA), video monitor.
8. Calcium (Ca<sup>2+</sup>) imaging: Light source (e.g., X-Cite, XLED1, Excilitec Technologies, Waltham MA, USA or Axon DG4), cooled CCD camera (e.g., Princeton Instruments, Trenton, NJ, USA, Microview model 1317 × 1035pixel format or TILL Imago QE cooled interline CCD, 1376 × 1040 pixel), software (e.g., Metafluor, Molecular Devices).

## **2.2 Material for In Vivo Recordings**

1. Anesthesia for mice C57/bl6: ketamine, 100 mg/kg; xylazine, 10 mg/kg; and atropine, 0.1 mg/kg).
2. Dental drill (Dremel, Racine, WI).
3. Stereotactic setup.
4. NaCl solution for rinsing.
5. Dental cement.
6. Cotton swab.
7. EtOH for disinfection of electrodes, metal screws, and surgical equipment.
8. Electrodes for MUA recordings, 2 twisted insulated stainless steel wires, 125 μm diameter, cut to 8 mm length plus one non-insulated ground electrode 125 μm diameter cut to 4 mm length (Plastics One, M333/3-B).
9. Electrode pedestal forming the connector for the electrodes.

10. Preamplifier, custom-made (INA 101 AM, Burr-Brown; gain,  $\times 10$  and AC amplifier band-pass, 500 Hz to 5 kHz; gain,  $\times 10,000$ ). Alternatively, preamplification can be used close to the head connector.
11. Window discriminator (custom-made or NeuroLog).
12. Power-1401 data acquisition (CED Instruments) using Sipke-2 software.
13. Recording cage with swivel/commutator (Plastics One, SL3 + 3C) and counterbalance.

---

## 3 Methods

### 3.1 Acute SCN Brain Slices

#### 3.1.1 General Features of SCN Slices

The acutely isolated brain slice has the advantages of offering accessibility and control while at the same time preserving many of the synaptic connections of the SCN circuitry. Previous workers have reported that the phase of the rhythms expressed in the SCN brain slice is predicted well by the prior LD cycle. For these reasons, it is an excellent *ex vivo* preparation to characterize synaptic communication in the SCN and to search for diurnal (i.e., day versus night) variations. The first concern in the use of acute SCN brain slices is the duration of time for which neural activity can be recorded. For the majority of brain regions, brain slices seem to remain healthy for 6–12 h. Due to this technical limitation, most experiments look for day–night variation by comparing properties of SCN neurons prepared in the day with those prepared during the night. For these experiments, animals are placed in constant conditions and the behavioral rhythm with wheel running activity. The brain slice can then be prepared at different phases of the daily cycle to evaluate circadian regulation. The same basic procedure for the preparation of brain slices is used for extracellular or intracellular sharp microelectrode or whole-cell patch-clamp recordings and  $\text{Ca}^{2+}$  imaging experiments.

#### 3.1.2 Methods for Generating SCN Slices

Animals are kept in LD regimes for a time sufficient to synchronize or entrain their circadian rhythm. Entrainment is typically achieved within 2–3 weeks, but it is advisable to validate the phase of the circadian clock of the animal at the time of preparation by monitoring the animal's locomotor activity rhythm. This is essential when using manipulations of the LD cycle, such as shifting the phase in a "jet lag" experiment or switching to constant darkness. The animals are killed by decapitation at times determined by the LD cycle ("Zeitgeber" time, ZT) or the behavioral rhythms (subjective or circadian time, CT). The effect of the time of preparation itself on the subsequent phase of the rhythm in electrical activity is small [23, 24], but caution should be taken when slices are prepared at night. Procedures need to be performed either in dim far-red light or under infrared (IR) illumination with the help of an IR viewer.

The brain slice procedures that we use are similar to those previously described [25–28]. Successful recording requires fast removal of the brain. The longer the time between decapitation and submersion of the brain into the ice-cold slice solution, the poorer the quality of the neurons in terms of resting membrane potential and other properties. The goal is to complete this part of the procedure in 1–2 min. Similarly, the success rate in long-term (>24 h) recordings of acute brain slices is improved by minimizing the total time it takes to transfer the slices to the recordings chamber (4–6 min). It is also critical to cut the optic nerves very carefully in an early stage of dissection to prevent any strain on the optic chiasm during preparation. For students learning this approach, pulling or tearing the optic nerves during the dissection is one of the most reasons for poor outcome. Specifically, brains are dissected and placed for ~1 min in ice-cold carbogenated (95% O<sub>2</sub>, 5% CO<sub>2</sub>) modified (ACSF) containing less CaCl<sub>2</sub> (1 mM) and more MgCl (5 mM) to inhibit synaptic transmission and reduce excitatory amino acid toxicity. After trimming the brain to a block of tissue containing the hypothalamus, a vibratome (e.g., Microslicer, DSK Model 1500E, Ted Pella, Redding, CA, USA) is used for making coronal slices with a thickness of 250–350 μm for patch-clamp and Ca<sup>2+</sup> imaging experiments under visual control. Successful sectioning of SCN slices using the vibratome requires a firm attachment of the brain to the cutting block. This is a common problem for beginners. If the brain moves when the blade hits the tissue, you will face difficulties. Therefore, a thin, even layer of cyanoacrylate is applied to the bottom of the vibratome chamber and the trimmed brain is glued to the cutting block with the optic chiasm facing the blade (*see Note 1*). The right combination of forward speed of the knife, vibration frequency, and, if applicable, amplitude of oscillation is critical for cutting smoothly through the tissue. Brains from older mice or especially rats require slower forward speed and higher frequency oscillation of the blade.

For >24 h MUA recordings of electrical activity from SCN neurons, a tissue chopper (McIlwain Tissue Chopper, The Mickle Laboratory Engineering, Guildford, UK) is preferred over a vibratome to minimize the time of preparation and produce 400–500 μm thick slices. Brain slices containing the SCN are then placed for at least 1 h before recording in our standard ACSF. This superfusate has a pH of 7.2–7.4 due to continuous gassing with carbogen while the osmolarity ranges between 290 and 300 mOsm. Patch-clamp and Ca<sup>2+</sup> imaging experiments can be performed at room temperature (22–25 °C), but slices need to be warmed up to 36 °C for 30 min right after cutting to activate endopeptidases. For MUA recordings, slices are immediately transferred to a recording chamber that is continuously superfused (1.5 ml/min) with warm (35.5 °C) oxygenated ACSF with added

antibiotic (gentamycin, 40 mg/ml). SCN slices are mechanically stabilized with either a metal fork or a nylon grid, preventing movement but allowing for access for recording electrodes.

While most acute slices will be used for a short period of time, the analysis of circadian rhythms requires longer recording times (at least 32 h). The cultured slice/organotypic explant would be more appropriate for longer recording times, but the acute slice offers many advantages when interested in photic entrainment and resetting mechanisms. To optimize the time that acute slices stay healthy in the recording dish, conditions must be as stable as possible (*see Note 2*). We have used several techniques to analyze the cellular or circuit properties of the SCN in an acute brain slice preparation. In the next section, we will briefly describe the techniques that we have found most useful for the analysis of the circadian circuit.

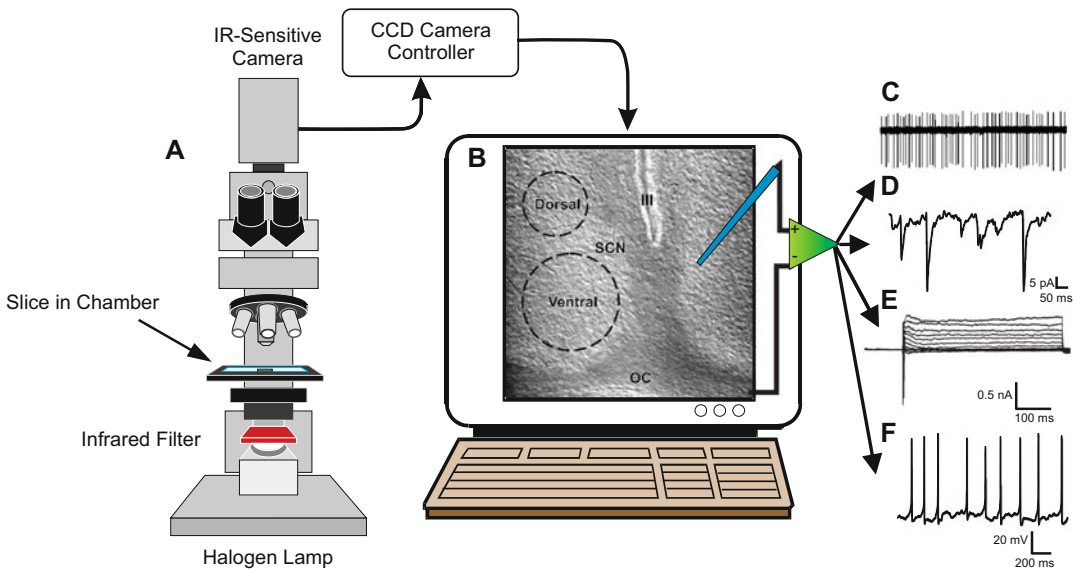


**Fig. 1** Patch-Clamp recordings from SCN brain slices. **(a)** Upright-microscope equipped with infrared-differential interference contrast (IR-DIC) and an IR-sensitive camera. Brain slice is placed in a recording chamber on the microscope stage. **(b)** Computer-controlled image processing showing IR DIC image of the mouse SCN. We have labeled the regions that we take to be dorsal or ventral in our experiments. The third ventricle (III) and optic chiasm (OC) are used as references. Most of our electrophysiological recording in the brain slice are made using this imaging technology to localize the recording site. **(c)** Recording of action potentials in cell-attached voltage-clamp mode with zero current injected. **(d)** Postsynaptic membrane currents. **(e)** Whole-cell voltage-dependent currents recorded as a response to a series of voltage steps. On the left, Na<sup>+</sup> inward current (downward reflections) and transient K<sup>+</sup> outward currents are visible. At the end of the pulses, the current consists mainly of steady state K<sup>+</sup> current. **(f)** Current-clamp recording of action potentials

### 3.2 Optical Approaches

#### 3.2.1 IR-DIC Videomicroscopy

Videomicroscopy allows for visualization of live, unstained cells in brain slice preparations [29, 30]. The brain slice rests in a perfusion chamber and is illuminated with IR light. Images are taken with differential interference contrast (DIC) optics and contrast-enhanced video microscopy. Figure 1a shows a view of SCN neurons in a brain slice as seen with IR-DIC videomicroscopy. The optic chiasm, third ventricle, and SCN are clearly visible. At higher magnification, it is possible to distinguish the borders and major processes of cells from the surface to about 150  $\mu\text{m}$  deep into a brain slice. This imaging technology is capable of targeting specific cells for electrophysiological analysis. The experimenter can clearly identify cells of the SCN and even distinguish different cell populations within the SCN. In addition, IR-DIC microscopy has improved the frequency of successful recordings and allows for the careful visual positioning of iontophoretic and stimulating electrodes. These are significant technological advantages for this type of study.

#### 3.2.2 $\text{Ca}^{2+}$ Imaging

$\text{Ca}^{2+}$  imaging techniques allow for dynamic measurements of  $\text{Ca}^{2+}$  levels inside neurons and have been particularly important in understanding the relationship between membrane events and

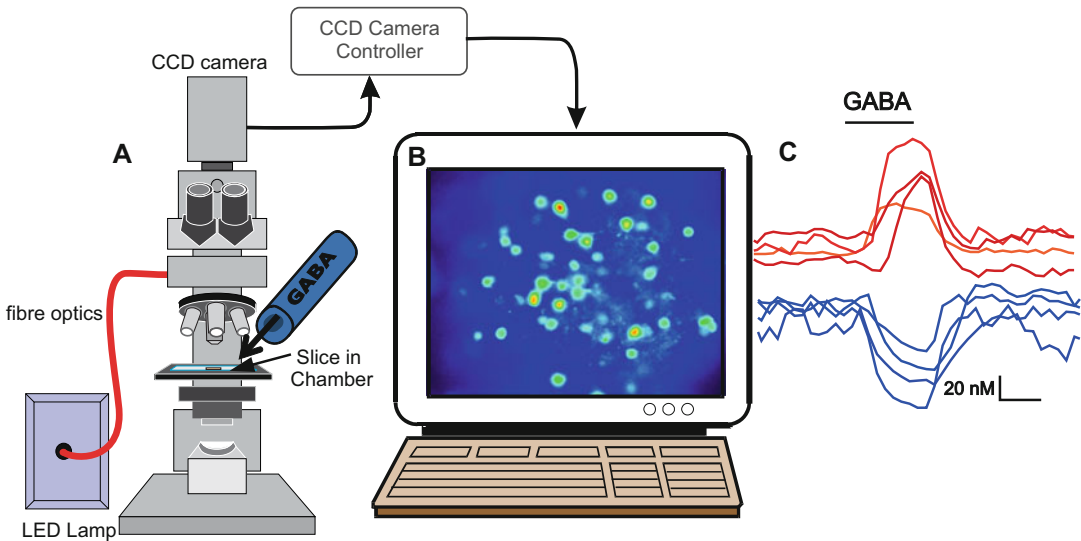


**Fig. 2** Calcium imaging to record cell responses to neurotransmitter agonist. (a) Fluorescent microscope using an LED lamp for excitation light coupled into the microscope light path by fiber optics. Images are recorded by a cooled CCD camera mounted at the microscope. Focal pressure application of neurotransmitter agonists—like GABA—can be performed through a quartz cannula (100  $\mu\text{m}$ ) (b) Computer-assisted imaging software controls light exposure, drug administration and image processing. Shown are Fura-2 AM-labeled SCN neurons which were imaged with a 40 $\times$  water immersion objective. (c) Right panel shows GABA-induced  $\text{Ca}^{2+}$  transients, which indicate that in the SCN some cells respond with “excitatory” responses (red lines) and some with “inhibitory” responses (blue lines). The true nature of the responses has to be confirmed with electrophysiological techniques

transcriptional regulation within the SCN. Furthermore, these techniques are useful in recording the neuronal response in a neuronal network to brief applications of neurotransmitters or other agents [31] (Fig. 2). To carry out  $\text{Ca}^{2+}$  imaging in the brain slice, we use a cooled charge-coupled device (CCD) camera (Princeton Instruments, Microview model 1317  $\times$  1035 pixel format, Trenton, NJ, USA) that is added to the Olympus fixed stage microscope. Two different methods are used to load the dye. In the first approach, slices are incubated in 10  $\mu\text{M}$  of the membrane-permeant acetoxymethyl (AM) form of the  $\text{Ca}^{2+}$ -sensitive fluorescent dye Fura-2 (Fura-2 (AM); Invitrogen, Life Technologies, Carlsbad, CA, USA) at 37 °C for 10 min (*see Note 3*). In a recent modification of this technique [32, 33], the SCN slice is exposed briefly (1 min) to stock solution of fura-2-AM (1 mM) and subsequently loading is continued for 1 h at room temperature using the diluted fura-2-AM in ACSF (10  $\mu\text{M}$ ). We used this modified loading protocol successfully in older rats (6 month) and old mice (2 years). The alternative approach uses membrane-impermeable fura-2 (1 mM pentapotassium salt) which is loaded into cells via the whole-cell-recording patch pipette [33]. The fluorescence of Fura-2 (AM) is excited alternatively at wavelengths of 357 nm and 380 nm by means of a high-speed wavelength switcher (1.2 ms switching capability, Sutter, Lambda DG-4, Novato, CA, USA). With the optics in many microscope objectives, there is a big difference in the transmission of light at 340 and 380 nm. This makes it difficult to bring fluorescence measurements from both 340 nm and 380 nm into the dynamic range of the camera. Accordingly, the dye can be excited with 357 nm light instead of 340 nm in these experiments. Image analysis software (MetaFluor, Universal Imaging, Molecular Devices, Sunnyvale, CA, USA) allows for the selection of several “regions of interest” within the field from which measurements of dynamic changes of Fura-2-(AM) fluorescence intensity are taken. To minimize bleaching of the dye, the intensity of excitation light and sampling frequency should be kept as low as possible.

Studies with Fura-2 (AM) are technically easy but have potential problems. Firstly, it is not possible to confidently resolve from which cell types (neurons vs. glia) the data are collected. Secondly, in practice, it appears to be more difficult to load cells in slices from older animals and, like with all AM-dyes applied via the bath, only cells located at the surface of the slice take up the dye. Loading dye via the patch pipette can solve these problems. However, this approach is much more laborious and it may be best to use this technique only when necessary to confirm a result obtained with the membrane-permeant form of this dye. Although Fura-2 is the standard dye we use for ratiometric  $\text{Ca}^{2+}$  measurements, there are some good arguments for employing other dyes. We have made

some use of the visible light  $\text{Ca}^{2+}$  indicator Oregon Green BAPTA (Invitrogen, Life Technologies, Carlsbad, CA, USA), Fluo-2 (TEFLabs, Austin TX, USA) as well as CAL-520 AM (Abcam, Cambridge, UK or AAT Bioquest, Sunnyvale, CA, USA). We obtain good loading of SCN slices with both dyes and one should see less phototoxicity. The use of visible rather than UV excitation should produce less autofluorescence. Since the cells in the SCN are known to undergo daily rhythms in metabolism, the possibility of daily rhythms in autofluorescence must be considered although we have found that autofluorescence is responsible for less than 5% of the signal. Finally, there are good arguments for the use of 2-photon laser scanning microscopy (2PLSM). 2PLSM offers several important advantages compared to conventional fluorescent microscopy with the CCD camera. All forms of imaging in thick brain tissue are limited by light scatter and longer wavelength light scatters less than shorter wavelength light. For this reason, the ability of the 2PLSM to make use of long wavelength light offers significant advantages for the resolution of structures deep in a brain slice. Furthermore, in 2PLSM the indicator dye is excited in a nonlinear manner. The requirement for two near coincident photons to achieve excitation of the dye means that only focused light reaches the required intensities and that scattered light does not excite the dye. This nonlinear excitation results in a significant reduction in photodamage and bleaching. This reduction in the damage caused by the excitation light is likely to be a critical advantage for experiments that involve taking measurements of  $\text{Ca}^{2+}$  for extended periods of time.

For the measurements using Fura-2, the free concentration of cytosolic  $\text{Ca}^{2+}$  can be calculated from the ratio ( $R$ ) of fluorescence intensities at 357 and 380 nm, using the following equation:  $[\text{Ca}^{2+}] = K_d \times \text{Sf} \times (R - R_{\min}) / (R_{\max} - R)$  [34]. Value for  $K_d$  is set at 135 nM, while values for  $R_{\min}$  and  $R_{\max}$  are determined with both in vitro and in vivo calibration methods. Initially, the in vitro method is used to make estimate values. With this method, rectangle glass capillaries are filled with high  $\text{Ca}^{2+}$  (Fura-2 + 10 mM  $\text{Ca}^{2+}$ ), low  $\text{Ca}^{2+}$  (Fura-2 + 10 mM EGTA) and a control saline without Fura-2. The fluorescence ( $F$ ) at 380 nm excitation of the low  $\text{Ca}^{2+}$  solution is imaged and the gain of the camera adjusted to maximize the signal. These camera settings will then remain fixed and background subtracted measurements made with 380 and 357 nm excitation of the three solutions:  $R_{\min} = F_{357 \text{ nm in low } \text{Ca}^{2+}} / F_{380 \text{ in low } \text{Ca}^{2+}}$ ;  $R_{\max} = F_{357 \text{ in high } \text{Ca}^{2+}} / F_{380 \text{ in high } \text{Ca}^{2+}}$ ;  $\text{Sf} = F_{380 \text{ in low } \text{Ca}^{2+}} / F_{380 \text{ in high } \text{Ca}^{2+}}$ . For the more accurate calibration methods [35], cells are loaded via the patch pipette using solutions inside the electrode similar to the normal internal solution but containing either no  $\text{Ca}^{2+}$  (20 mM EGTA) or 10 mM  $\text{Ca}^{2+}$  for  $R_{\min}$  and  $R_{\max}$ , respectively. To obtain estimates of the

effective  $K_d$ , three different EGTA/ $\text{Ca}^{2+}$  solutions are used with calculated free  $\text{Ca}^{2+}$  of 111 nM (10 mM EGTA/3.5 mM  $\text{Ca}^{2+}$ ), 207 nM (10 mM EGTA/5 mM  $\text{Ca}^{2+}$ ), and 483 nM (10 mM EGTA/7 mM  $\text{Ca}^{2+}$ ). By calibrating in the slice preparation with solutions of ionic strength similar to those used for measurements, some of the uncertainties associated with calibration of  $\text{Ca}^{2+}$  indicators can be avoided.

### 3.3 Electrophysiological Approaches

#### 3.3.1 Long-Term Multiunit and Single-Unit Extracellular Recordings

Extracellular electrical activity of SCN neurons in freshly prepared brain slice can be measured by extracellular glass, metal, or suction electrodes. Glass microelectrodes have been used to record the neuronal activity of single SCN neurons for short times (typically <20 min). The accumulative data of repeated measurements represent the activity of the population of SCN neurons [36–38]. This method is rather labor-intensive, but can be useful to determine neural activity at peak or trough of the daily rhythm. The use of stationary metal electrodes (Fig. 3) allows for the automated continuous recording of MUA for longer than 24 h [39]. Electrodes are fabricated from platinum/iridium wire ( $\phi$  50–75  $\mu\text{m}$ ), which are mechanically stabilized within glass capillaries, electrically isolated by resin and polished at the tip. The use of suction electrodes has

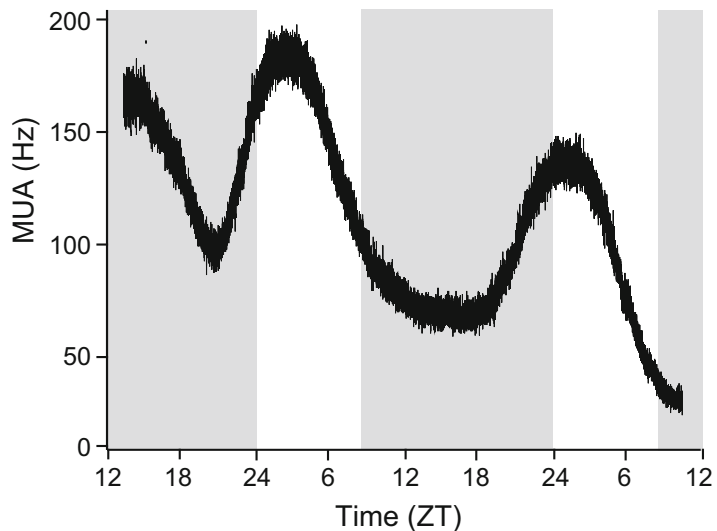


**Fig. 3** Rhythms in multiunit activity (MUA) recorded in mouse SCN. Acute SCN brain slices exhibit a typical circadian rhythm in spontaneous electrical activity with peak activity during the mid of the projected light phase (mid-subjective day) and low activity during the projected dark phase (mid-subjective night). The animal has been subjected to a short-day photoperiod (8 h light, 16 h dark) for 30 days prior to preparing the brain slice. Photoperiod “memory” is reflected in the narrow peak of the SCN activity matching the short light phase. Gray and white background indicate darkness and light of the previous light regime. Time is expressed in Zeitgeber time with 0 defined as the beginning of the light phase

been described showing stable long term recordings of SCN neuronal activity (up to 92 h) and a good yield of distinguishable single units in the MUA signal [40]. MUA recordings with stationary electrodes require extremely stable conditions for slice, perfusion and electrode placement.

Slices are placed on a nylon mesh fixed on a metal platform grid made from titanium or platinum. The platform is mounted in a diamond-shaped chamber optimized for laminar flow of the bath medium. The bath level is adjusted to 0.1 mm above the slice surface and held stable throughout the experiment. A peristaltic pump provides even inflow of medium into the chamber and a steel cannula (18 gauge needle) placed perpendicular to the surface and connected to a regulated vacuum aspirates the medium at the other end of the flow-through chamber. The chamber is mounted on a vibration-damped table inside a faraday cage. Metal or suction electrodes as well as the slice hold-down are placed with the help of micromanipulators (e.g., MM33, Märzhäuser, Wetzlar, Germany). Neuronal signals are amplified and bandwidth-filtered (e.g., Signal Recovery 5113, AMETEK, Wokingham, UK; [41]). Action potentials with signal-to-noise ratio of 2:1 (noise <5  $\mu$ V from baseline) are selected by spike triggers and counted electronically every 10 s. The positions of the electrodes and spike trigger settings should not be changed during the experiment. Data analysis of MUA includes smoothing of raw data to determine the phase of the peak and trough of the electrical activity rhythm. Peak width of the MUA waveforms can be determined between the upward and downward flank at the half maximum frequency, representing the duration of the electrical circadian output signal generated by the SCN.

For isolation of single units from MUA data, the complete waveform of action potentials above a given threshold is digitized and recorded (Power-1401 data acquisition and Spike-2 software, CED, Cambridge, UK). Offline analysis of spike parameters (amplitude, latency) is used to validate distinct spike waveforms in a cluster analysis [41]. Putative single units identified in distinct clusters are verified displaying an event-free refractory period (0–50 ms) in the interspike interval histogram. Similar to MUA data, single unit firing rate can be binned and plotted over time. The timing and width of the single-unit activity pattern are calculated on smoothed data.

### 3.3.2 Sharp *Microelectrode Recording*

Sharp microelectrode techniques were used in the initial analysis of the physiology of SCN neurons by Kim and Dudek [42] but have not been used much recently. Intracellular recordings of membrane potential or currents are obtained from SCN neurons using glass microelectrodes filled with 3 M K-acetate. DC resistances typically vary from 70 to 100 M $\Omega$ . The signals are amplified by an active bridge circuit amplifier (Axoclamp 2A, Molecular Devices,

Sunnyvale, CA, USA) amplifier in bridge or current clamp mode). After a neuron is impaled, a baseline recording is obtained to ensure that the cell's membrane properties are stable. This baseline membrane potential is maintained throughout the course of the experiment by manually adjusting the DC current. Hyperpolarizing DC current pulses (0.3–0.4 nA, 50 ms duration, 0.5 pulses/s repetition rate) were applied throughout all experiments to monitor conductance changes. The cell's membrane properties are monitored every 10 min by determining its current–voltage relationship by injection of depolarizing and hyperpolarizing pulses (100 ms duration); the cell's input resistance is determined from the linear portion of the current–voltage plots. Membrane excitability is also measured as the response of the neuron to depolarizing current pulses (0.1 nA steps, 500 ms duration). Electrophysiological information on the effects of experimental treatments on action potential and after hyperpolarization duration and amplitude is obtained by analyzing the first action potential evoked by the current pulses. “P Clamp” software (Molecular Devices, Sunnyvale, CA, USA) is used for data analysis.

### 3.3.3 *Whole-Cell Patch-Clamp Recording*

The methods for patch-clamp recording are similar to those described previously [12, 25, 28, 31, 43]. Slices are placed in a custom designed chamber attached to the fixed stage upright microscope. The slice is held down with thin nylon threads glued to a platinum wire and submerged in continuously flowing, oxygenated ACSF (25 °C) at 2 ml/min. Recording whole-cell currents in voltage-clamp with patch electrodes from visually identified cells in 350  $\mu\text{m}$  thick slices is a standard procedure in our research group. This method provides a number of important advantages over “blind patch” and “thin slice” techniques. Individual neurons can be visualized up to 150  $\mu\text{m}$  below the surface of the slice using IR-differential interference contrast (IR-DIC) optics (Fig. 1b). Thus, the recording pipette can be aimed at a particular cell. In the SCN, this means that specific cells populations can be targeted for electrophysiological analysis. Visualization also permits more accurate placement of iontophoretic pipettes and stimulating electrodes. The thicker slice (250–350  $\mu\text{m}$ ) also makes tissue handling easier than with 120–150  $\mu\text{m}$  thin slices. Furthermore, the synaptic physiology can be studied because much of the local connectivity remains intact in these thicker slices (Fig. 1d). Subsequent staining with biocytin permits more precise cell identification of the dendritic processes. A disadvantage of this preparation is the necessity for using tissue from younger animals. Cells are best visualized in slices from animals of less than P30. Although cells can be visualized up to and beyond P60 (in mice), in the older tissue it is more difficult to clearly distinguish cells especially deeper into the tissue. Whole-cell recordings also tend to be of better quality in tissue less than P30.

Electrodes are pulled on a multistage puller (e.g., Sutter P-97; 1.5 mm o.d. borosilicate capillary glass, Sutter Instrument, Novato, CA, USA or Narishige PC-10). Patch electrode resistances in the bath are typically 3–6 M $\Omega$  when filled with standard “intracellular” solution (*see* below). Whole-cell recordings are obtained with an Axon Instruments 200B amplifier and monitored online with pCLAMP (Ver. 6.0, Axon Instruments, Molecular Devices, Sunnyvale, CA, USA). To minimize changes in offset and/or liquid junction potentials with changing ionic conditions, the ground path uses an ACSF agar bridge to a Ag/AgCl ground well. Cells are approached with slight positive pressure (20–30 mm H<sub>2</sub>O) and offset potentials are corrected. The pipette is lowered to the vicinity of the membrane keeping a positive pressure. After forming a high resistance seal (2–10 G $\Omega$ ) by applying negative pressure, cell-attached recording of action potentials in voltage-clamp mode can be performed (Fig. 1c). Holding potential should be adjusted so no current is passing through the pipette to obtain reliable values for spontaneous firing frequency. Subsequently, a second (fast) pulse of negative pressure is used to break the membrane. While entering the whole-cell mode, a repetitive test pulse of 10 mV is delivered to the cell in a passive potential range (holding at –60 to –70 mV). Once the whole-cell recording configuration is established, whole-cell capacitance is estimated integrating current transients produced voltage steps according to standard methods. Whole-cell capacitance and electrode resistance are neutralized and compensated (50–80%) using the pulse. Data acquisition is then initiated. In voltage-clamp mode, whole-cell ion currents can be measured (Fig. 1d) and in current-clamp mode, membrane voltage can be recorded to obtain information of action potential frequency and waveform as well as postsynaptic potentials (Fig. 1e). The series and input resistances are monitored throughout the experiment by checking the response to small pulses in a passive potential range. Data should be rejected, if series resistance is greater than 20 M $\Omega$  or if either value changes significantly (>20%) during the course of the experiment.

The extracellular solutions used will vary according to the goals of the experiment. The standard solution is described above. When necessary, various combinations of ionic solutions plus specific blocking agents are used to maximize the presence of a particular ion current under study current and minimize the presence of others. Solution exchanges within the slice are achieved by a rapid gravity feed delivery system. In our system, the effects of bath-applied drugs begin within 15 s and are typically complete by 1–2 min. The composition of the internal solutions used to isolate different intrinsic currents (if necessary), ligand-gated, or synaptic currents will also vary according to the particular conditions and goals of the experiment. The standard solution in the patch pipette

contains (in mM): 125 Cs-methanesulfonate, 9 EGTA, 8 HEPES, 8 MgATP, 4 NaCl, 3 KCl, and 1 MgCl<sub>2</sub>. The pH of this solution is adjusted to 7.25–7.3 and the osmolality is between 280 and 290 mOsm. In some experiments, in which activity of voltage-sensitive Ca<sup>2+</sup> channels is studied GTP (1 mM), phosphocreatine (10 mM), and leupeptin (0.1 mM) was added. With this internal solution, stable Ca<sup>2+</sup> currents can be recorded for up to 30 min. EGTA is omitted from the experiments using the patch electrode to load calcium indicators.

A common concern in voltage-clamp electrophysiological experiments is the adequacy of the space-clamp in cells in slices, that is, the ability to maintain voltage control of the membrane at sites distant to the recording electrode. For most studies using this technique, the ability to maintain voltage control can be improved by the blockade of most voltage-gated currents and the use of cells from younger tissue which do not have large dendritic trees. Maintenance of reasonably good space-clamp is difficult in older cells with larger amplitude currents. For all cells, smooth transitions in the current–voltage relationships can be used as indicators of good voltage control. In addition, any cell which shows a high series resistance (>20 MΩ) or tail currents which do not decay rapidly with a single exponential should not be used. It is important to be aware of these problems and carefully monitor the adequacy of space clamp conditions. Another technical concern is that while the whole-cell patch-clamp technique offers improved voltage control, it also dialyzes the inside of the cell. This can result in the loss of membrane currents that are, for example, highly dependent upon phosphorylation. One solution to this problem is, for comparison, to run some experiments with sharp-electrode intracellular recording techniques and without ion channel blockers. An alternative possibility is to use the “perforated patch” technique [26].

### 3.3.4 Evoked EPSCs and Stimulation Techniques

Electrical stimulation can be used to induce local excitatory postsynaptic currents (EPSCs) that are mediated by ionotropic glutamate receptors [25, 43]. Local stimulation is applied with bipolar electrodes constructed from twisted Teflon-coated silver wires (0.2 mm diameter exposed at the tip, tip separation 0.2–0.5 mm). The electrode is placed 0.5–1.0 mm from the recording pipette. Constant current square pulses (50–1000 μA intensity, 10–100 μs duration, 1 pulse/4–5 s) are used to induce short latency, graded amplitude EPSCs. In some cases, the stimulation frequency can be increased to 100 Hz. This should induce temporally summated long-duration EPSCs which will likely have a larger NMDA component. The threshold for EPSC onset is determined and a series of intensities from just above threshold for the EPSC to maximum amplitude is used. Changes in EPSC characteristics are determined prior to and at selected intervals after drug administration. Local

stimulation activates cut input and output fibers as well as local neurons. There is a component of the EPSC mediated by activation of GABA<sub>A</sub> receptors when the stimulus is applied in the SCN. To reduce the contribution of activation of GABA<sub>A</sub> receptors, the blocker gabazine can be added to the ACSF. To prevent action potentials, QX-314 (20 mM) can be used in the recording pipette. The bath application of specific glutamate receptor antagonists (e.g., AP5 or CNQX) can be used to produce EPSCs mediated mainly by activation of NMDA or AMPA/KA receptors. The optic nerve is stimulated with the use of a custom-made suction electrode; constant current pulses (biphasic square wave) of 0.1–1.0 mA intensity and 0.5–2.0 ms duration are applied at 30 s intervals.

### 3.4 *In Vivo Methods*

#### 3.4.1 *Animals*

As discussed, it is critical to house the animals in a robust LD cycle for at least 2 weeks prior to the experiments. Mice are housed individually, and food and water are available ad libitum. Running wheels were often provided prior to the experiments, and running discs can be used as an alternative during the recordings (*see Note 4*).

#### 3.4.2 *Experimental Setup*

In vivo equipment for measuring SCN activity in freely moving mice requires a well-designed, dedicated system. The mouse is recorded within a Faraday cage and is connected to a cable but must be able to move in all directions (Fig. 4). The in vivo measurement system has been constructed in a way that it is causing the least possible tension to the mouse by neutralizing the weight of the cable and headstage. This ensures minimal impact on the behavior of the mouse. SCN neurons produce very small extracellular electrical signals, due to the extremely small size of the cells (~10 μm). The small signals are buffered (impedance correction or preamplified), and subsequently fed into a differential amplifier. The in vivo setup allows for stable recordings from an animal for a long time. This is important for recording long-lasting effects of changes in photoperiod [41] or exposure to constant light [5–7].

If the recordings are to be made on moving animals, the in vivo physiological system will require a swivel and balancing system. The swivel consists of a slip ring (Moog or Moflon) mounted with a set of small ball bearings in a light-weight housing (26 g custom-made). The design should ensure very low friction, a low signal noise and a long life. In addition, a swivel balancing system is required. The swivel balancing system compensates the weight of the swivel with cable and follows the vertical movement of the mouse. With a damped long spring, the balancing system ensures a very smooth balance and minimal friction at the onset of the animal's movement. It is based on a long spring with contra weights (custom-made).

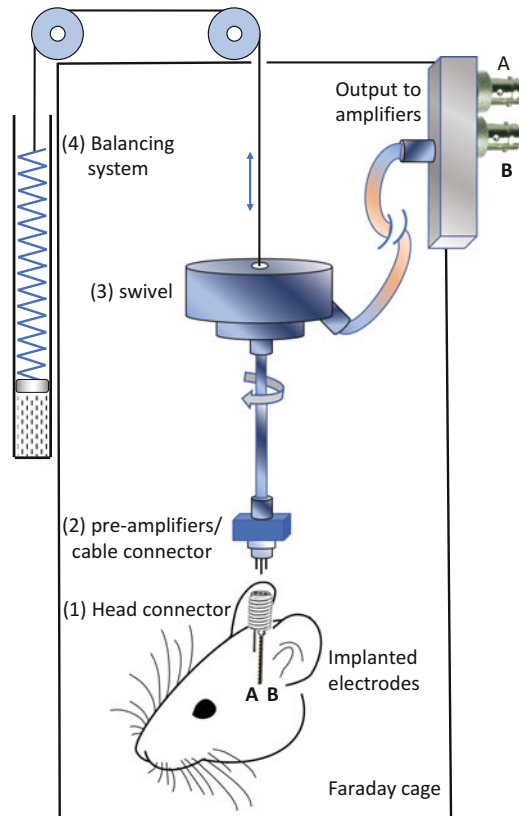


**Fig. 4** Schematic diagram of an *in vivo* SCN recording setup. The implanted electrodes (1) are attached to the head via a customized connector. The preamplifiers in the head connector (2) are custom-built in our lab and are designed to have extremely low noise (below  $9 \text{ nV}/\sqrt{\text{Hz}}$  at 1 kHz), low input current leakage ( $<10 \text{ pA}$ ), and small size ( $7 \times 3 \text{ mm}$ ). A custom-built swivel/commutator (3) provides an extremely smooth 7–8 channel slip ring (Moog or Moflon), long life, low noise, extremely low-friction movement, and a lightweight housing (total weight: 26 g). The swivel balancing system (4) counterbalances the weight of the swivel, preamplifiers, and the cable. Finally, a damped long spring ensures smooth movements, which is essential when recording from a rapidly moving rodent

### 3.4.3 *In Vivo* Electrode Placement

Electrodes are insulated stainless steel,  $125 \mu\text{m}$  twisted electrodes (Plastics One). The third electrode is used as a reference (ground). The three electrodes end up in a 3-pole female connector (MS333, Plastics One). The male connector fits on the head connector and has two built-in preamplifiers and swivel cable (Plastics One/custom-made).

Mice are anaesthetized using a mix of ketamine ( $100 \text{ mg/kg}$ ), xylazine ( $20 \text{ mg/kg}$ ), and atropine ( $1 \text{ mg/kg}$ ). The electrodes are implanted under a  $5^\circ$  off the vertical axis to prevent hitting the blood sinus. In C57bl/6 mice, the coordinates are  $0.46 \text{ mm}$

posterior to bregma 0.14 mm lateral to midline and 5.38 mm ventral to the dura mater. The details of these coordinates vary someone with the strain of mice, the position of the toothbar and the stereotaxic device. The electrode is fixed to the skull using three screws and dental cement.

#### 3.4.4 Recording

After a week of recovery from surgery, animals are placed in a custom-designed recording chamber to measure SCN electrical activity simultaneously with behavioral activity using passive infra-red sensors. Animals are connected to the recording system using a counterbalanced swivel system in which they are able to freely move. The electrical signal is amplified and bandwidth filtered (0.5–5 kHz). Window discriminators are used to convert action potentials into digital pulses that are counted in 2 s epochs. The neural activity in the SCN is typically recorded under both LD and DD condition. Many SCN neurons are light-responsive, and this can be used to confirm placement of the electrode into the SCN.

#### 3.4.5 Signal Processing

The use of preamplifiers close to the recording site enhances the signal to noise ratio and differential amplification reduces movement artifacts. The two SCN signals are buffered by two small operational amplifiers (opamps) mounted close to the head of the mouse on the cable connector. These pre-amplifiers are selected for low input current leakage (*see Note 5*). The noise of the pre-amplifiers should be much lower than the noise level generated by the thermal noise of the electrodes. A low input current leakage is necessary, otherwise the electrode tip may degenerate in time and the SCN signal will decrease.

The two buffered SCN signals, A and B, are connected to the inputs of a differential amplifier. This device only amplifies the difference between two input voltages but suppresses any voltage common to the two inputs:  $\text{output} = (A-B) \times \text{Gain}$ . This amplifier should also be a low noise type because the signal level for in vivo recording is extremely low. The gain of the amplifier will be low because DC biopotentials may exist between the electrodes and should be eliminated by a high pass filter. Therefore, the gain should be about 10–20 times. Latest-generation differential amplifier ICs have low noise levels which allows for more amplification to be done earlier in the recording process. Common mode signals are signals that are present in both inputs so that they are eliminated by the differential amplifier:  $A-B$ . Signals like movement artifacts, cable noise, or electrical interference will also be reduced that way. After this stage, further filtering and amplification of the signal will be applied.

### 3.4.6 Analysis

Analysis of electrophysiological data is a big topic that requires more detailed consideration than we can provide here, as it depends on the aim of the experiment (analysis of population activity; of single units, or of single units simultaneously, etc.). In general, the electrophysiological signals of SCN activity are first digitized at 25 kHz using Spike2 hardware and software (Cambridge Electronic Design) and stored for offline analysis. The digitized recordings are imported into MATLAB as “waveform data,” including data from light and movement sensors, using parts of the sigTOOLSON Library (<http://sigtool.sourceforge.net>). Imported waveform data are triggered at fixed voltage amplitude settings (e.g., for the analysis of electrical activity patterns of separate neuronal populations), and time and amplitude of these action potentials are used for the analysis of single units.

### 3.4.7 Histology to Confirm Electrode Placement

At the end of each recording, a small negative current (3–5  $\mu\text{A}$ ; 3–5 min) is passed through the microelectrode to mark the recording site while perfusion with 4% paraformaldehyde solution containing ferrocyanide. The animals are sacrificed and brain tissue collected for histological verification of the electrode location. Brains are sectioned coronally and stained with cresyl violet. The ferrocyanide will leave a blue precipitate at the electrode tip, as a result of the small negative current. The position of the electrode can be determined by microscopic inspection. Electrodes outside the SCN are excluded from analysis. Some type of histological confirmation of electrode placement is a critical control for these experiments.

---

## 4 Summary of Results on the SCN Network and Future Directions

As neuroscientists, an essential goal of our research is to understand how the nervous system works at all levels of organization. We now understand several basic principles underlying the properties of neurons and their synaptic interconnections. We can accurately describe neural interactions, and in many cases, we can use imaging techniques to know what brain regions are active in driving specific particular behaviors. Still, there is a giant gap in our understanding of how behaviors emerge from neurons and the circuits they form. Filling this gap requires an understanding of how neurons organized in circuits and networks generate the complex interactions of electrical and chemical signals that ultimately generate rhythmic behaviors.

The overall goal of our research is to understand the cellular and circuit-level properties of neurons that generate circadian rhythms. Circadian rhythms offer a special opportunity for a study of neural circuits. Although individual neurons can generate the basic periodicity, other properties emerge from interactions within

local circuits [3, 4]. To study this circuit, we are attempting to develop a set of *ex vivo* circadian models of increasing cellular complexity, from single cells to geometrically defined assemblies of oscillator neurons that make up the intact system. We hope to study how the canonical properties of circadian clocks emerge through multioscillator interactions. Much of the resources and efforts in the field of circadian rhythms have been devoted to understanding the molecular genetic mechanisms that underlie these oscillations. We feel that the field of chronobiology would benefit from expanding its focus on genetic mechanisms to include more work on how molecular rhythms drive rhythms in electrical activity, how the SCN circuit functions as an ensemble, and how this ensemble is impacted with aging and disease. In order to affect this expansion, we need to bring together the insights and talents of neuroscientists from a number of backgrounds including anatomy, physiology, and modeling. New insights emerging from outside of the field seem likely. The partnership between more physiologically oriented scientists with those with quantitative/model expertise is likely to pay dividends, and indeed, this has started to occur [44–46]. Hopefully, our experience with the *in vitro* and *in vivo* analysis of the SCN, as described in this chapter, will help bridging the electrophysiological to the molecular studies as well as to the development of quantitative models.

---

## 5 Notes

1. The cyanoacrylate (superglue) used to fix the brain to the cutting chamber of the vibratome can form filaments when ACSF is poured into the chamber. This can impede cutting when these filaments are located between the blade and the brain tissue. Avoid this by dripping a few drops of ACSF onto the brain before filling the chamber.
2. Some of the problems that can occur and jeopardize long-term recordings are fluctuating bath fluid level, condensation due to temperature differences and fluctuations in ambient temperature, mechanically instable slice tissue or electrodes, salt formation at the aspiration needle and fluctuations in the vacuum.
3. The synthetic AM dyes used as intracellular  $\text{Ca}^{2+}$  probes are highly hydrophilic. Since access of the dye to the cell membrane is necessary for loading, the loading medium often contains a dispersant like Pluronic (TefLabs F-127). We and others [47] found that a concentration of 1–10% Pluronic in DMSO and a DMSO concentration of 0.25–0.7% in the ACSF yield the most effective dye loading.

4. Running wheels are often provided to the animal before the recording. We have evidence that this can positively affect rhythm amplitude and animal health.
5. The opamps used should be selected based on the following criteria: (1) very low noise: below 9 nV/ $\sqrt{\text{Hz}}$  at 1 kHz; (2) very high input impedance; (3) very low input current leakage: <10 pA; and (4) very small footprint (TSSOP):  $6.6 \times 3$  mm (for 2 opamps).

## References

1. Schaap J, Pennartz CM, Meijer JH (2003) Electrophysiology of the circadian pacemaker in mammals. *Chronobiol Int* 20:171–188
2. Colwell CS (2011) Linking neural activity and molecular oscillations in the SCN. *Nat Rev Neurosci* 12:553–569
3. Welsh DK, Takahashi JS, Kay SA (2010) Suprachiasmatic nucleus: cell autonomy and network properties. *Annu Rev Physiol* 72:551–577
4. Meijer JH, Michel S (2015) Neurophysiological analysis of the suprachiasmatic nucleus: a challenge at multiple levels. *Methods Enzymol* 552:75–102
5. Meijer JH, Watanabe K, Schaap J, Albus H, Detari L (1998) Light responsiveness of the suprachiasmatic nucleus: long-term multiunit and single-unit recordings in freely moving rats. *J Neurosci* 18:9078–9087
6. van Oosterhout F, Fisher SP, van Diepen HC, Watson TS, Houben T, VanderLeest HT et al (2012) Ultraviolet light provides a major input to non-image-forming light detection in mice. *Curr Biol* 22:1397–1402
7. van Diepen HC, Foster RG, Meijer JH (2015) A colourful clock. *PLoS Biol* 13:e1002160
8. van Oosterhout F, Lucassen EA, Houben T, vanderLeest HT, Antle MC, Meijer JH (2012) Amplitude of the SCN clock enhanced by the behavioral activity rhythm. *PLoS One* 7:e39693
9. Kudo T, Block GD, Colwell CS (2015) The circadian clock gene *Period1* connects the molecular clock to neural activity in the suprachiasmatic nucleus. *ASN Neuro* 7:1759091415610761
10. Meijer JH, Colwell CS, Rohling JH, Houben T, Michel S (2012) Dynamic neuronal network organization of the circadian clock and possible deterioration in disease. *Prog Brain Res* 199:143–162
11. Farajnia S, Deboer T, Rohling JH, Meijer JH, Michel S (2014) Aging of the suprachiasmatic clock. *Neuroscientist* 20:44–55
12. Itri J, Colwell CS (2003) Regulation of inhibitory synaptic transmission by vasoactive intestinal peptide (VIP) in the mouse suprachiasmatic nucleus. *J Neurophysiol* 90:1589–1597
13. Choi HJ, Lee CJ, Schroeder A, Kim YS, Jung SH, Kim JS et al (2008) Excitatory actions of GABA in the suprachiasmatic nucleus. *J Neurosci* 28:5450–5459
14. Kuhlman SJ, McMahon DG (2006) Encoding the ins and outs of circadian pacemaking. *J Biol Rhythm* 21:470–481
15. Colwell CS (2000) Circadian modulation of calcium levels in cells in the suprachiasmatic nucleus. *Eur J Neurosci* 12:571–576
16. Ikeda M, Sugiyama T, Wallace CS, Gompf HS, Yoshioka T, Miyawaki A et al (2003) Circadian dynamics of cytosolic and nuclear  $\text{Ca}^{2+}$  in single suprachiasmatic nucleus neurons. *Neuron* 38:253–263
17. O'Neill JS, Maywood ES, Chesham JE, Takahashi JS, Hastings MH (2008) cAMP-dependent signaling as a core component of the mammalian circadian pacemaker. *Science* 320:949–953
18. Brancaccio M, Maywood ES, Chesham JE, Loudon AS, Hastings MH (2013) A Gq- $\text{Ca}^{2+}$  axis controls circuit-level encoding of circadian time in the suprachiasmatic nucleus. *Neuron* 78:714–728
19. Abe M, Herzog ED, Yamazaki S, Straume M, Tei H, Sakaki Y et al (2002) Circadian rhythms in isolated brain regions. *J Neurosci* 22:350–356
20. Lamont EW, Robinson B, Stewart J, Amir S (2005) The central and basolateral nuclei of the amygdala exhibit opposite diurnal rhythms of expression of the clock protein *Period2*. *Proc Natl Acad Sci U S A* 102:4180–4184
21. Wang LM, Dragich JM, Kudo T, Odom IH, Welsh DK, O'Dell TJ et al (2009) Expression of the circadian clock gene *Period2* in the hippocampus: possible implications for synaptic

- plasticity and learned behaviour. *ASN Neuro* 1: e00012
22. Granados-Fuentes D, Ben-Josef G, Perry G, Wilson DA, Sullivan-Wilson A, Herzog ED (2011) Daily rhythms in olfactory discrimination depend on clock genes but not the suprachiasmatic nucleus. *J Biol Rhythm* 26:552–560
  23. Gillette MU (1986) The suprachiasmatic nuclei: circadian phase-shifts induced at the time of hypothalamic slice preparation are preserved in vitro. *Brain Res* 379:176–181
  24. vanderLeest HT, Vansteensel MJ, Duindam H, Michel S, Meijer JH (2009) Phase of the electrical activity rhythm in the SCN in vitro not influenced by preparation time. *Chronobiol Int* 26:1075–1089
  25. Colwell CS (2001) NMDA-evoked calcium transients and currents in the suprachiasmatic nucleus: gating by the circadian system. *Eur J Neurosci* 13:1420–1428
  26. Itri JN, Michel S, Vansteensel MJ, Meijer JH, Colwell CS (2005) Fast delayed rectifier potassium current is required for circadian neural activity. *Nat Neurosci* 8:650–656
  27. Itri JN, Vosko AM, Schroeder A, Dragich JM, Michel S, Colwell CS (2010) Circadian regulation of A-type potassium currents in the suprachiasmatic nucleus. *J Neurophysiol* 103:632–640
  28. Michel S, Itri J, Han JH, Gnietczynski K, Colwell CS (2006) Regulation of glutamatergic signalling by PACAP in the mammalian suprachiasmatic nucleus. *BMC Neurosci* 7:15
  29. MacVicar BA (1984) Infrared video microscopy to visualize neurons in the in vitro brain slice preparation. *J Neurosci Methods* 12:133–139
  30. Dodt HU, Zieglansberger W (1994) Infrared videomicroscopy: a new look at neuronal structure and function. *Trends Neurosci* 17:453–458
  31. Farajnia S, van Westering TL, Meijer JH, Michel S (2014) Seasonal induction of GABAergic excitation in the central mammalian clock. *Proc Natl Acad Sci U S A* 111:9627–9632
  32. Farajnia S, Meijer JH, Michel S (2015) Age-related changes in large-conductance calcium-activated potassium channels in mammalian circadian clock neurons. *Neurobiol Aging* 36:2176–2183
  33. Irwin RP, Allen CN (2007) Calcium response to retinohypothalamic tract synaptic transmission in suprachiasmatic nucleus neurons. *J Neurosci* 27:11748–11757
  34. Gryniewicz G, Poenie M, Tsien RY (1985) A new generation of  $Ca^{2+}$  indicators with greatly improved fluorescence properties. *J Biol Chem* 260:3440–3450
  35. Neher E (1995) The use of fura-2 for estimating  $Ca^{2+}$  buffers and  $Ca^{2+}$  fluxes. *Neuropharmacology* 34:1423–1442
  36. Groos G, Hendriks J (1982) Circadian rhythms in electrical discharge of rat suprachiasmatic neurones recorded in vitro. *Neurosci Lett* 34:283–288
  37. Green DJ, Gillette R (1982) Circadian rhythm of firing rate recorded from single cells in the rat suprachiasmatic brain slice. *Brain Res* 245:198–200
  38. Jiang ZG, Yang Y, Liu ZP, Allen CN (1997) Membrane properties and synaptic inputs of suprachiasmatic nucleus neurons in rat brain slices. *J Physiol* 499(1):141–159
  39. Albus H, Bonnefont X, Chaves I, Yasui A, Doczy J, van der Horst GT et al (2002) Cryptochrome-deficient mice lack circadian electrical activity in the suprachiasmatic nuclei. *Curr Biol* 12:1130–1133
  40. Brown TM, Banks JR, Piggins HD (2006) A novel suction electrode recording technique for monitoring circadian rhythms in single and multiunit discharge from brain slices. *J Neurosci Methods* 156:173–181
  41. VanderLeest HT, Houben T, Michel S, Deboer T, Albus H, Vansteensel MJ et al (2007) Seasonal encoding by the circadian pacemaker of the SCN. *Curr Biol* 17:468–473
  42. Kim YI, Dudek FE (1991) Intracellular electrophysiological study of suprachiasmatic nucleus neurons in rodents: excitatory synaptic mechanisms. *J Physiol* 444:269–287
  43. Kim YI, Choi HJ, Colwell CS (2006) Brain-derived neurotrophic factor regulation of N-methyl-D-aspartate receptor-mediated synaptic currents in suprachiasmatic nucleus neurons. *J Neurosci Res* 84:1512–1520
  44. Mirsky HP, Liu AC, Welsh DK, Kay SA, Doyle FJ 3rd (2009) A model of the cell-autonomous mammalian circadian clock. *Proc Natl Acad Sci U S A* 106:11107–11112
  45. Vasalou C, Herzog ED, Henson MA (2009) Small-world network models of intercellular coupling predict enhanced synchronization in the suprachiasmatic nucleus. *J Biol Rhythm* 24:243–254
  46. Hu K, Meijer JH, Shea SA, vanderLeest HT, Pittman-Polletta B, Houben T et al (2012) Fractal patterns of neural activity exist within the suprachiasmatic nucleus and require extrinsic network interactions. *PLoS One* 7:e48927
  47. Hamad MI, Krause M, Wahle P (2015) Improving AM ester calcium dye loading efficiency. *J Neurosci Methods* 240:48–60